

5.4 CIRRUS CLOUD ICE WATER CONTENT IN THE UPPERMOST TROPOSPHERE: SIX YEARS OF OBSERVATIONS FROM THE CLOUD AND AEROSOL LIDAR WITH ORTHOGONAL POLARIZATION

Melody A. Avery^{1,*}, A. J. Heymsfield², D. M. Winker¹, M. Vaughan¹, S. A. Young³, and C. Trepte¹
¹NASA/LARC, Hampton, VA; ²NCAR, Boulder, CO; ³CSIRO/MAR, Aspendale, VIC, Australia

1. INTRODUCTION

The purpose of this paper is to provide an overview description of the global cloud ice water content product provided by the first long-term space lidar mission. The Cloud and Aerosol Lidar with Orthogonal Polarization (CALIOP) has been providing data from the Cloud-Aerosol Lidar and Infrared Pathfinder Satellite Observation (CALIPSO) satellite for more than six years, since June, 2007. Figure 1 is a schematic representation of CALIPSO with CALIOP operating as part of the NASA A-Train. CALIPSO is host to three co-aligned nadir-viewing instruments; these are CALIOP (lidar), as well as the Imaging Infrared Radiometer (IIR) and Wide Field Camera (WFC). CALIOP provides a suite of cloud and aerosol data products, including ice water content (IWC), ice water path (IWP), cloud particle extinction and optical depth (OD). The IIR also provides cloud data products, including IWP, OD, effective diameter and a microphysical parameter that diagnoses cloud particle habit. Data from the three instruments on CALIPSO are synergistic since they provide perfectly collocated information about the clouds below the satellite. An overview of the CALIPSO mission is available in Winker et al. (2010).

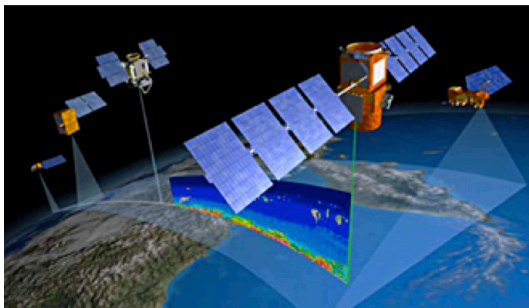


Figure 1: Schematic representation of CALIOP operation on the CALIPSO satellite in the NASA A-Train satellite constellation.

*Corresponding author: Melody Avery
melody.a.avery@nasa.gov, 757-864-5522

Due to space limitations this paper discusses only the CALIOP cloud IWC observations, while recognizing that there are critical contributions and synergy from the IIR and WFC on CALIPSO. CALIOP is a two-wavelength elastic backscatter lidar that operates at 532 and 1064 nm, with a cross-polarized signal also available at 532 nm. More information about the lidar can be obtained in Hunt et al. (2009). The fundamental CALIOP cloud property measurements are two-way transmittance through the cloud layer, attenuated backscatter, and depolarization ratio, all using the 532 nm channels. Figure 2 shows an example of CALIOP attenuated backscatter measured on the western side of the Hurricane Sandy “super-storm” of 2012.

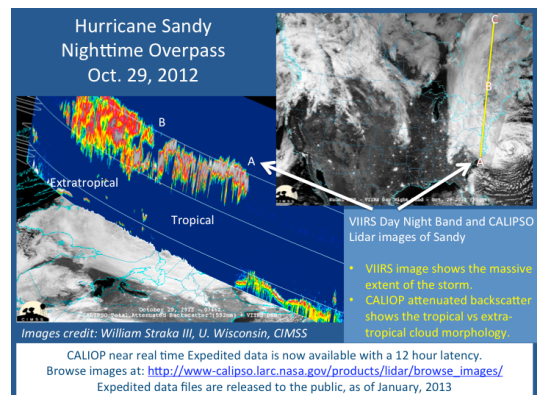


Figure 2: Hurricane Sandy CALIPSO overpass, with expedited data available in near-real time.

The CALIOP backscatter “curtain” is shown combined with the VIIRS day/night image of Sandy just before landfall, and shows the difference between the tropical and extratropical ice cloud microphysics and structure. All CALIPSO data is available in near-real time (“Expedited”) for forecast model evaluation, emergency management and fieldwork, and as climate data records for publication, research and for climate model evaluation. Two links to CALIPSO

data and browse images are: a) <http://www-calipso.larc.nasa.gov/products>
and b) <http://www.icare.univ-lille1.fr/archive>

Cloud particle ice water content is derived from CALIOP attenuated backscatter as described in the next section. Climate and other atmospheric models diagnose and predict ice water content (IWC) to calculate radiative and latent heating, and for total water budgets. Clouds and cloud feedbacks are currently the largest source of uncertainty in climate models, which are lacking global cloud IWC data for model validation (Waliser, 2009). Currently climate model cloud IWC estimates differ by factors of between 0.03 and 15 times a reference IWC standard (Jiang et. al., 2012)

2. ICE WATER CONTENT PARAMETERIZATION

CALIOP IWC is calculated from attenuated backscatter using a multi-step process. First an automated processor (Vaughan et. al., 2009) identifies cloud layers, and produces total 532 nm backscatter for the cloud layer. Extinction is then retrieved using the backscatter or, when there is enough signal, it is calculated from the measured two-way transmittance through the cloud (Young and Vaughan, 2009). Finally, IWC is parameterized using an empirical relationship between visible extinction and IWC derived from numerous *in situ* and remote aircraft-based measurements (Heymsfield et. al., 2005). The equation that describes the extinction (σ) and IWC relationship used to produce CALIOP Version 3 IWC is:

$$IWC = a\sigma^b, a=119, b=1.22 \quad (1)$$

Figure 3 illustrates these steps for the Sandy overpass, with a) Total 532 nm backscatter, b) Extinction and c) IWC. The differing tropical (LHS) and extra-tropical (RHS) ice cloud morphology is also evident in this series of plots.

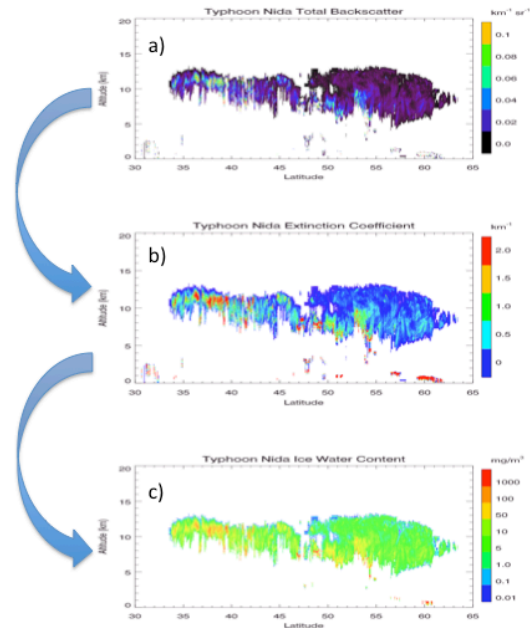


Figure 3: Building CALIOP IWC from backscatter measurements: example from Sandy.

3. ICE WATER CONTENT COMPARISONS

With a view towards establishing the accuracy and reliability of the CALIOP IWC product, a rigorous validation is being performed by comparison with other IWC observations, both from aircraft field campaigns and from other satellite instruments. Shown here are examples of two types of comparisons; a case study and some global statistics. Many more detailed comparisons and analysis are currently being performed. A preliminary example of validation efforts is published in Avery et. al. (2012).

3.1 Three Views of Typhoon Nida

The NASA A-Train also contains the CloudSat satellite with a Cloud Profiling Radar (CPR) instrument that also makes profile measurements of cloud properties. Because CALIOP and CPR provide the first long-term (more than six years) set of collocated cloud profiles, it is important to understand the relationship between the radar and lidar measurements. Both instrument teams provide an IWC product, and there are also two combined radar and

lidar IWC retrievals available called "2C-ICE" (Deng and Mace, 2010) and "DARDAR" (Delanoe et al, 2011). CloudSat data is not available for the nighttime Sandy overpass shown in the previous section, so a case study of Typhoon Nida, a major tropical cyclone in the Pacific basin in 2009, is shown here. Tropical cyclones provide informative case studies because they ordinarily contain a large dynamic range of IWC. Figure 4 shows a MODIS infrared image of Typhoon Nida and the CPR (bottom) and CALIOP (RHS) measurements of reflectivity and attenuated backscatter.

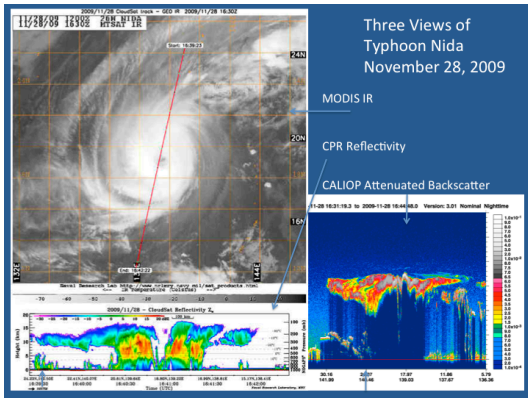


Figure 4: MODIS, CloudSat CPR and CALIPSO CALIOP views of Typhoon Nida.

The radar and lidar observations both have limitations. The radar does not detect small ice particles, which tend to occur at the top and southeastern side of Nida. The lidar signal is attenuated in thick clouds, which occur in the cyclone core and on the northwestern side. The combined IWC retrieval uses both the lidar and the radar to show the complete structure of Nida.

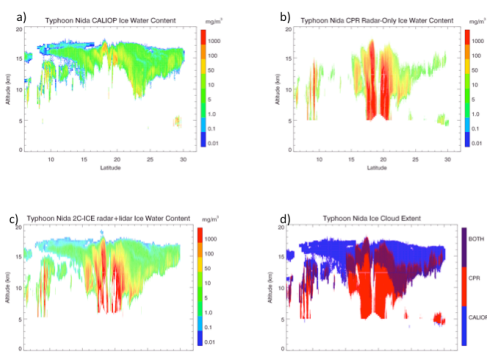


Figure 5: Comparison of Typhoon Nida Ice Water Content; lidar, radar and combined.

Figure 5 shows the resulting ice water content from a) the lidar only, b) the radar only, and c) from the combined 2C-ICE retrieval. Figure 5d maps the spatial coverage of the two instruments, with lidar-only in blue, radar-only in red, and the overlap region in purple. This spatial distribution gives some information about the storm: the region in blue has small ice particles with IWC less than about 5 mg/m^3 . The region in red has an optical depth that is greater than about 3. CALIOP data also provides depolarization, which gives information about cloud particle phase and habit, while CPR data provides rainfall information.

3.2 Global Intercomparisons

In addition to case studies, global statistical comparisons are needed to build confidence in the IWC products from satellite instruments. Accurate IWC measurements are difficult from airplanes, and perhaps even more so from satellites. Even though we cannot conclusively prove which satellite data set is correct, agreement between two or more satellite instrument data sets increases confidence in the observations.

Figure 6 shows a three-way comparison of global IWC data between 55°S and 55°N , between CALIOP, CPR and 2C-ICE. First the CALIOP and CPR data is volume-matched, and only bins are selected that have both valid and non-zero CALIOP and CPR data. This is the overlap region shown in purple for the Nida example, but determined over most of the globe.

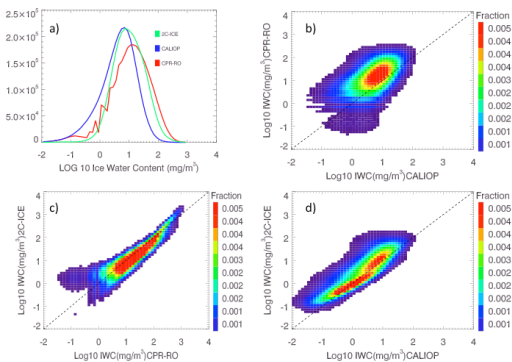


Figure 6: Global comparison of radar, lidar and combined IWC retrievals, January, 2008.

The histograms in Figure 6a show that the CPR IWC is higher than CALIOP IWC in the matched regions, with the 2C-ICE combined retrieval in between. 2C-ICE shows a peak in the IWC distribution that is more similar to CALIOP, but does not capture the smaller values of IWC. CPR and 2C-ICE see IWC larger than 100 mg/m^3 that isn't detected by CALIOP. Currently the CALIOP team is refining the extinction retrieval algorithm and IWC parameterization for Version 4, and the newer version will likely show better agreement between the radar and lidar observations.

Figure 7 shows a comparison between CALIOP IWC and IWC retrieved by the Microwave Limb Sounder (MLS) on the AURA satellite, also part of the A-Train. One objective of Figure 7 is to show how viewing geometry can affect how satellite instruments view clouds and also how comparisons are interpreted. The first two panels in the figure show Typhoon Nida, from CALIOP (a) and from MLS (b). The lidar has a 70 m beam diameter and 60 m vertical resolution, and the single-shot data is averaged over 5 km. The MLS has a limb viewing geometry, and vertical averaging functions that result in a spatial resolution of approximately $300 \times 7 \times 4 \text{ km}^3$ (Wu *et al.*, 2009). CALIOP resolves the details of IWC distribution within the storm, while MLS averages Nida's IWC into large bins.

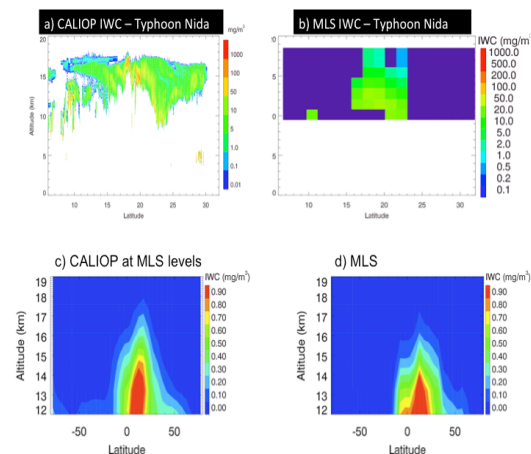


Figure 7: Comparisons of CALIOP and MLS IWC.

Both MLS and CALIOP have a similar sensitivity to IWC of about 0.1 mg/m^3 , and both measure in the upper troposphere and

lowermost stratosphere, consequently the zonally averaged IWC shown in the bottom two panels compares very well. Here the CALIOP data has been averaged to match the MLS sample volume. This comparison suggests that the CALIOP data is representative of global upper troposphere, even though the lidar sample volume is limited.

Column-integrated CALIOP IWC was also compared with MODIS Collection 5 ice water path (Figure 8). The relationship between cloud ice water path (IWP) and OD is the same as that between IWC and extinction, but integrated over the column for comparison with passive sensors. This comparison shows that the MODIS ice water path amounts are consistently larger than the CALIOP integrated IWC. These results are consistent with comparisons between the IIR effective optical depth (OD), CALIOP 532 nm OD and MODIS Collection 5 OD (Anne Garnier, personal communication). The effective infrared OD is expected to be 50% of the visible OD (Garnier *et al.*, 2012), and the IIR acts as a reliable transfer standard between CALIOP and MODIS. Tests of extinction retrievals being considered for the CALIOP V4 release not only improve comparisons to MODIS OD, but also improve the the CPR-CALIOP IWC comparisons. More work on both MODIS Collection 6 and CALIOP Version 4 is underway, but this initial test is encouraging and demonstrates how the satellite instruments can work together to improve difficult retrievals of cloud properties.

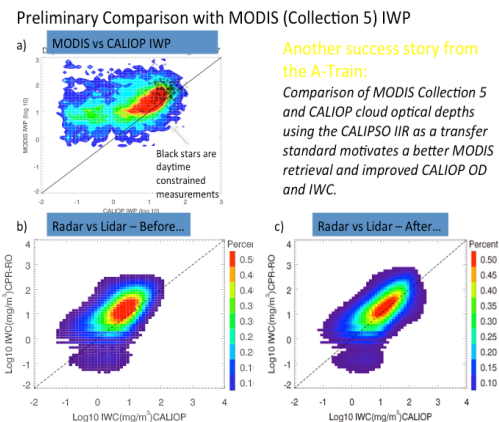


Figure 8: MODIS and CALIOP comparison results.

4. ICE WATER CONTENT DISTRIBUTION AND UNCERTAINTY

4.1 Global Distribution

One advantage of long-term satellite observations of clouds is that it allows for characterization of the mean global cloud distribution. Figures 9a-b show zonal averages of IWC and two-way transmittance, averaged to 1 km vertically, and into $1^\circ \times 1^\circ$ horizontal bins. A maximum in upper tropospheric IWC in the equatorial tropics is clear in the region of maximum convective outflow. The lidar uncertainty increases as the lidar signal becomes more attenuated in thick clouds, so the lidar data is most accurate at higher altitudes where the overhead two-way transmittance is high. From Figure 9b it can be seen that the average transmittance is 60% or greater at altitudes of 8 km and above. The lidar signal penetrates to significantly lower altitudes at high latitudes, so CALIOP also provides observations of polar IWC.

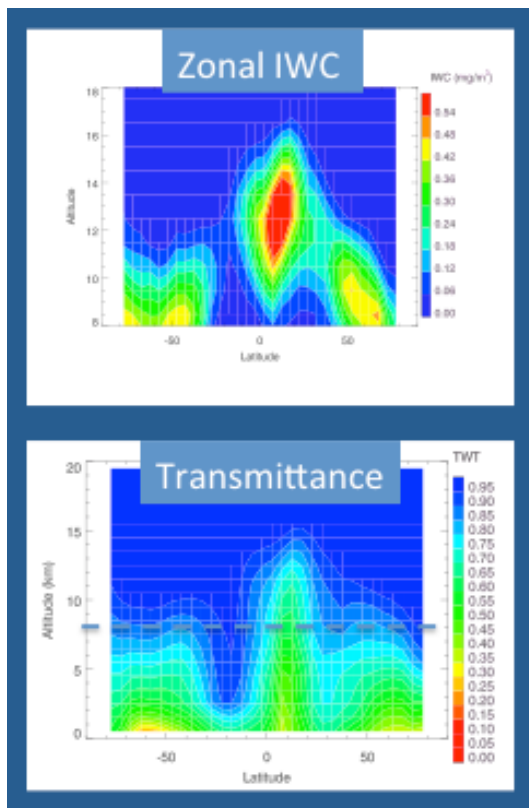


Figure 9: a) Zonally averaged ice water content measured by CALIOP for the month

of July, 2007. b) Two-way Transmittance measured by CALIOP, also July, 2007.

4.2 Sensitivity and Uncertainty

The CALIOP IWC uncertainty is determined by propagating the uncertainty in the extinction retrieval through the IWC parameterization. Figure 10a shows the relative error and Figure 10b shows the IWC uncertainty as a function of overhead two-way transmittance (TWT) as determined by the CALIOP Version 3 algorithm, which does not include the IWC parameterization uncertainty. The short dashed line on Figure 10b shows the point where the TWT falls below 60%. The large relative errors shown in pale blue at the right of 10a is mainly due to either very tenuous clouds with very small IWC amounts, or to a very small signal (small overhead TWT as shown on the LHS of Figure 10b). For a detailed description of the complex derivation of the extinction uncertainty, the reader is referred to Young et al. (2013). An additional 30-80% uncertainty is estimated to come from the IWC parameterization (Heymsfield et. al., manuscript in preparation).

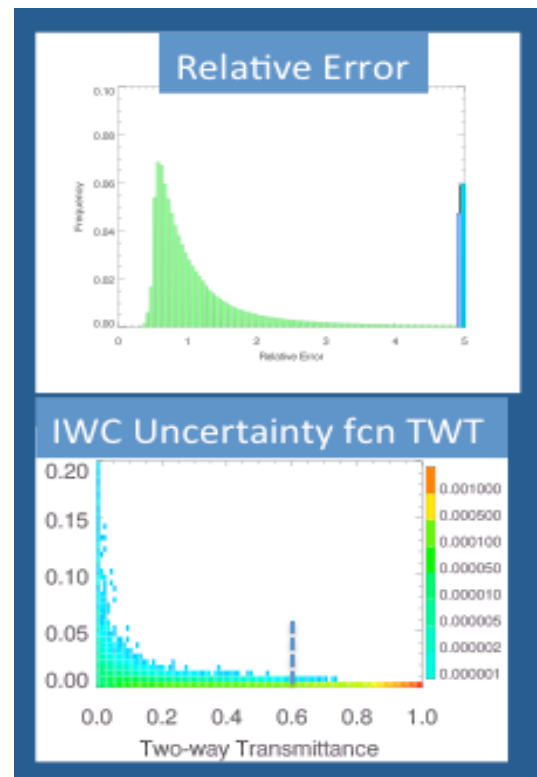


Figure 10: CALIOP ice water content relative error (a) and uncertainty versus overhead transmittance (b).

4.3 Asian Monsoon Time Series

Recently there has been much community interest in characterizing changes in cloud and aerosol distributions due to climate cycles, such as the Asian monsoon. CALIOP IWC observations now extend for more than six years, and CALIOP IWC sensitivity is sufficient to detect seasonal and annual changes in cloud distribution, particularly in the tropical upper troposphere and polar regions where cloud radiative forcing and feedbacks are a significant influence on climate. Figure 11 shows upper tropospheric IWC during five complete Asian monsoon cycles. Research into Asian monsoon cycle variability using CALIOP IWC data is ongoing, however Figure 11 shows that CALIOP data can capture the variation between monsoon cycles.

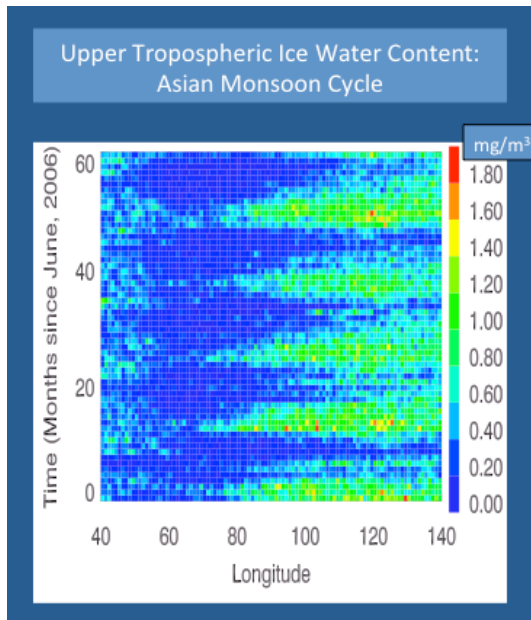


Figure 11: Five-year time series of upper tropospheric ice water content in the Asian Monsoon region, averaged to 1 degree horizontally and to 1 km vertically.

5. SUMMARY

CALIOP (CALIPSO lidar) provides a unique 3-D global view of mid and high-altitude tropical cloud ice water content, as well as IWC distribution information at lower altitudes in the subtropics, and at mid- and high-latitudes. CALIOP data is now available as an “expedited” data set in near-real time, and as a climate data record for

publication and research. Cloud ice water content is a reliable product, and the CALIPSO team is working to validate CALIOP cloud data products, specifically IWC, by comparison with *in situ* and other satellite data sets. Cloud ice water content accuracy is likely to be limited by the natural variability in cloud microphysical properties, however CALIOP IWC uncertainty is comparable to or lower than IWC derived from other satellite-based sensor data. CALIOP IWC data, together with CPR provides a global 3-dimensional IWC data set to inform climate and other atmospheric models, and to study cloud-related processes.

6. REFERENCES

- Avery, M., D. Winker, A. Heymsfield, M. Vaughan, S. Young, Y. Hu and C. Trepte (2012), “Cloud ice water content retrieved from the CALIOP space-based lidar”, *Geophys. Res. Lett.*, **39**, doi:10.1029/2011GL050545.
- Delanoë, J., R. J. Hogan, R. M. Forbes, A. Bodas-Salcedo and T. H. M. Stein, 2011: “Evaluation of ice cloud representation in the ECMWF and UK Met Office models using CloudSat and CALIPSO data”, *Q. J. Roy. Meteorol. Soc.*, **137**, 2064–2078, doi:10.1002/qj.882.
- Deng, M. and G. G. Mace, Z. Wang and H. Okamoto (2010), “Tropical Composition, Clouds and Climate Coupling Experiment validation for cirrus cloud profiling retrieval using CloudSat radar and CALIPSO lidar”, *J. Geophys. Res.*, **115**, D00J15, doi:10.1029/2009JD013104.
- Garnier, A., J. Pelon, P. Dubuisson, M. Faivre, O. Chomette, N. Pascal, and D. Kratz (2012), “Retrieval of cloud properties using CALIPSO imaging infrared radiometer, Part 1: Effective emissivity and optical depth”, *J. Ap. Met. And Clim.*, **51**, doi:10.1175/JAMC-D-11-0220.1.
- Heymsfield, A. D. Winker and G.-J. van Zadelhoff (2005), “Extinction-ice water content-effective radius algorithms for CALIPSO”, *Geophys. Res. Lett.*, **32**, L10807, doi:10.1029/2205GL022742.
- Hunt, W. H, D. M. Winker, M. A. Vaughan, K. A. Powell, P. L. Lucker, and C. Weimer, 2009: “CALIPSO Lidar Description and Performance Assessment”, *J. Atmos. Oceanic Technol.*, **26**, 1214–1228, doi:10.1175/2009JTECHA1223.1.

- Jiang, J. H., H. Su, C. Zhai, V. S. Perun, A. Del Genio, L. S. Nazarenko, L. J. Donner, L. Horowitz, C. Seman, J. Cole, A. Gettelman, M. A. Ringer, L. Rotstayn, S. Jeffrey, T. Wu, F. Brient, J.-L. Dufresne, H. Kawai, T. Koshiro, M. Watanabe, T. S. L'Ecuyer, E. M. Volodin, Trond Iversen, Helge Drange, M. D. S. Mesquita, W. G. Read, J. W. Waters, B. Tian, J. P. Teixeira, and G. L. Stephens (2012), "Evaluation of cloud and water vapor simulations in CMIP5 climate models using NASA "A-Train" satellite observations", *J. Geophys. Res.*, **117**, D14105, doi:10.1029/2011JD017237.
- Vaughan, M., K. Powell, R. Kuehn, S. Young, D. Winker, C. Hostettler, W. Hunt, Z. Liu, M. McGill, B. Getzewich, 2009: "Fully Automated Detection of Cloud and Aerosol Layers in the CALIPSO Lidar Measurements", *J. Atmos. Oceanic Technol.*, **26**, 2034–2050, doi: 10.1175/2009JTECHA1228.1.
- Waliser, D. E., J.-L. F. Li, C. P. Woods, R. T. Austin, J. Bachmeister, J. Chern, A. Del Genio, J. H. Jiang, Z. Kuang, H. Meng, P. Minnis, S. Platnick, W. B. Rossow, G. L. Stephens, S. Sun-Mack, W.-K. Tao, A. M. Tompkins, D. G. Vane, C. Walker, and D. Wu (2009), "Cloud Ice: A climate model challenge with signs and expectations of progress", *J. Geophys. Res.*, **114**, D00A21, 1-27, doi:10.1029/2008JD010015.
- Winker, D. M., J. Pelon, J. A. Coakley Jr., S. A. Ackerman, R. J. Charlson, P. R. Colarco, P. Flamant, Q. Fu, R. M. Hoff, C. Kittaka, T. L. Kubar, H. Le Treut, M. P. McCormick, G. Megie, L. Poole, K. Powell, C. Trepte, M. A. Vaughan, and B. A. Wielicki (2010), "The CALIPSO Mission: A Global 3D View of Aerosols and Clouds", *Bull. Am. Meteorol. Soc.*, *Sept. 2010*, 1211-1229.
- Winker, D. M., M. A. Vaughan, A. H. Omar, Y. Hu, K. A. Powell, Z. Liu, W. H. Hunt, and S. A. Young, 2009: "Overview of the CALIPSO Mission and CALIOP Data Processing Algorithms", *J. Atmos. Oceanic Technol.*, **26**, 2310–2323, doi:10.1175/2009JTECHA1281.1.
- Wu, D.L., J.H. Jiang, W.G. Read, R.T. Austin, C.P. Davis, A. Lambert, G.L. Stephens, D.G. Vane, and J.W. Waters (2008), "Validation of the Aura MLS Cloud Ice Water Content (IWC) Measurements", *J. Geophys. Res.* **113**, doi:10.1029/2007JD008931.
- Young, S. and M. Vaughan (2009), "The Retrieval of Profiles of Particulate Extinction from Cloud-Aerosol Lidar Infrared Pathfinder Satellite Observations (CALIPSO) Data: Algorithm Description", *J. Atmos. Oceanic Tech.*, **26**, 1105-1119, doi: 10.1175/2008JTECH1221.1
- Young, S. and M. Vaughan, R. Kuehn and D. Winker (2013), "The Retrieval of Profiles of Particulate Extinction from Cloud-Aerosol Lidar Infrared Pathfinder Satellite Observations (CALIPSO) Data: Uncertainty and Error Sensitivity Analyses" *J. Atmos. Oceanic Technol.*, doi: 10.1175/JTECH-D-12-00064.1